



Investigation of magnetite Fe_3O_4 nanoparticles for magnetic hyperthermia

Zbigniew Surowiec,
Arkadiusz Miaskowski,
Mieczysław Budzyński

Abstract. The paper presents the investigation of magnetic nanoparticles (MNPs) dedicated to hyperthermia application. The crystal structure and size distributions have been determined by means of transmission electron microscope (TEM) and X-ray diffraction (XRD). Magnetic properties of the nanoparticles were tested by Mössbauer spectroscopy together with calorimetric experiments. The Mössbauer spectroscopic study of MNPs revealed the existence of a superparamagnetic phase. The relative contribution of the relaxing component to the total spectrum at room temperature was about 10%. The heating effect of these MNPs under alternating magnetic field was examined. The temperature increase has reached 5°C in 10 min. The preliminary temperature rise suggests that the investigated materials are applicable for hyperthermia.

Keywords: Mössbauer effect • superparamagnetic nanoparticles • hyperthermia

Z. Surowiec[✉], M. Budzyński
Institute of Physics,
Maria Curie-Skłodowska University,
1 M. Curie-Skłodowskiej Sq., 20-031 Lublin, Poland,
Tel.: +48 81 537 6220, Fax: +48 81 537 6191,
E-mail: zbigniew.surowiec@umcs.lublin.pl

A. Miaskowski
Department of Applied Mathematics and Computer
Science,
University of Life Sciences in Lublin,
Lublin, Poland

Received: 14 July 2016
Accepted: 15 December 2016

Introduction

The use of magnetic nanoparticles (MNPs) in biomedical applications has increased considerably in the recent years [1–3]. Several applications of MNPs are reported in the literature, ranging from cell labeling [4] and drug targeting [5] to cancer treatment [6]. Currently, MNPs are being investigated for the use in hyperthermia, and it is called magnetic fluid hyperthermia (MFH).

MFH is based on the feeding of MNPs into tumour and then applying an external magnetic field of hundreds of kilohertz. The dissipation of magnetic field energy associated with the superparamagnetic particles can be explained based on the linear response theory (LRT) [7] in which two relaxation times associated with the Néel relaxation and the Brownian rotation of the particles are considered. Finally, the magnetic field energy is converted into heat and leads to a local temperature rise.

In this work, we undertake the systematic study of dimercaptosuccinic acid (DMSA)-coated magnetite nanoparticles in order to determine the relevant parameters involved in the power dissipation of MNPs i.e. the average particle size, the specific absorption rate (SAR), and the intrinsic loss parameter (ILP). Moreover, the characterization of the magnetic properties of MNPs with the Mössbauer spectroscopy measurements was discussed.

Experimental

The sample studied in this work was supplied by Liquids Research Ltd [8], i.e. DMSA-stabilized magnetite nanoparticles with dominant diameter of 10.3 nm dispersed in the water.

The heating properties of the liquid samples were examined using the nanoTherics MagneTherm system [9]. The applied frequency of magnetic field (f) was 273 kHz, and the magnetic field strength (H_{\max}) was 10.3 kA/m. The magnetic energy dissipation in the ferrofluid sample was measured using the thermodynamic relation expressed in terms of SAR and ILP as [10]

$$(1) \quad \text{SAR} = \frac{C \frac{dT}{dt} + L \cdot \Delta T}{m_{\text{MNP}}}$$

$$(2) \quad \text{ILP} = \frac{\text{SAR}}{f \cdot H_{\max}^2}$$

where C is the heat capacity of the sample, T is the temporal temperature, t is the time of measure, L is the constant that quantifies the proportionality between the temperature and the losses, and ΔT is the difference in temperature ($T - T_0$).

The other measurements were conducted with dried samples. The X-ray diffraction (XRD) patterns were measured by means of a Philips X'Pert PW 3040/60 using diffractometer with $\text{CuK}\alpha$ radiation at room temperature (RT). They were fitted using the FullProf program for the Rietveld refinement method. The ^{57}Fe Mössbauer spectra were measured in transmission geometry using a constant acceleration spectrometer with a $^{57}\text{Co}/\text{Rh}$ source. Experimental temperatures were controlled by Janis SVT Research Cryostat System. The isomer shift (IS) was calibrated against a metallic iron foil at RT.

Results

The type of the particles, their size distribution, and magnetic properties are very important qualities of MNPs used in magnetic hyperthermia. In order to determine the morphological and structural qualities, transmission electron microscopy (TEM) and XRD measurement were performed.

Figure 1 shows the TEM image of nanoparticles. First, one can see that the shape of nanoparticles is very regular, they have a spherical shape. Second, the nanoparticles are well separated. These particles do not connect with one another because they are coated with DMSA surfactant.

DMSA surfactant prevents nanoparticles aggregation, and additionally, it can be a linker that connects chemical molecules or antibodies in the hyperthermia [11].

In the inset of Fig. 1, the size distribution of nanoparticles is presented. The average size of the nanoparticles obtained based on the analysis of the TEM images is equal to 11.4 nm.

The XRD pattern of investigated sample is presented in Fig. 2. The pattern was analysed by means

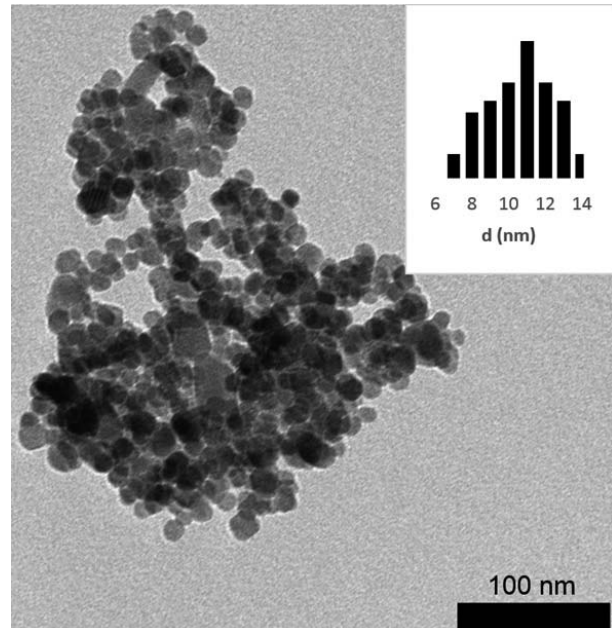


Fig. 1. The TEM image of the magnetite nanoparticle and particle size distribution.

of the Rietveld method. The sample was identified as Fe_3O_4 . The lattice constant (a) is equal to 8.366 Å, and it is less than the lattice constant for bulk magnetite. The size and the lattice strains of the nanoparticles were determined from the diffraction peak broadening by using the Williamson-Hall method [12]. The size of nanoparticles (d) determined by means of XRD is equal to 12.3 nm, and it is consistent with the size of the nanoparticles observed in TEM image. The lattice strains (η) are equal to 0.12% and, they are probably connected with surface layer of the nanoparticles. This layer is disordered and, what is more, not all atoms have complete surrounding.

Figure 3 shows the Mössbauer spectra of magnetite nanoparticles at various temperatures.

The pattern obtained at a temperature of 3 K consists of two sextets connected with Fe atoms located in tetrahedral and octahedral lattice. The intensity ratio between octahedral and tetrahedral site is equal to 1:2. With increasing temperature, essential modification of intensity ratio can be observed. At a temperature of 200 K, the contribution

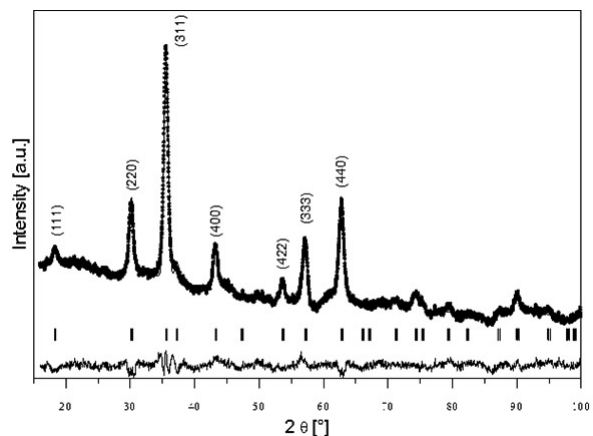


Fig. 2. The XRD patterns of nanoparticle Fe_3O_4 .

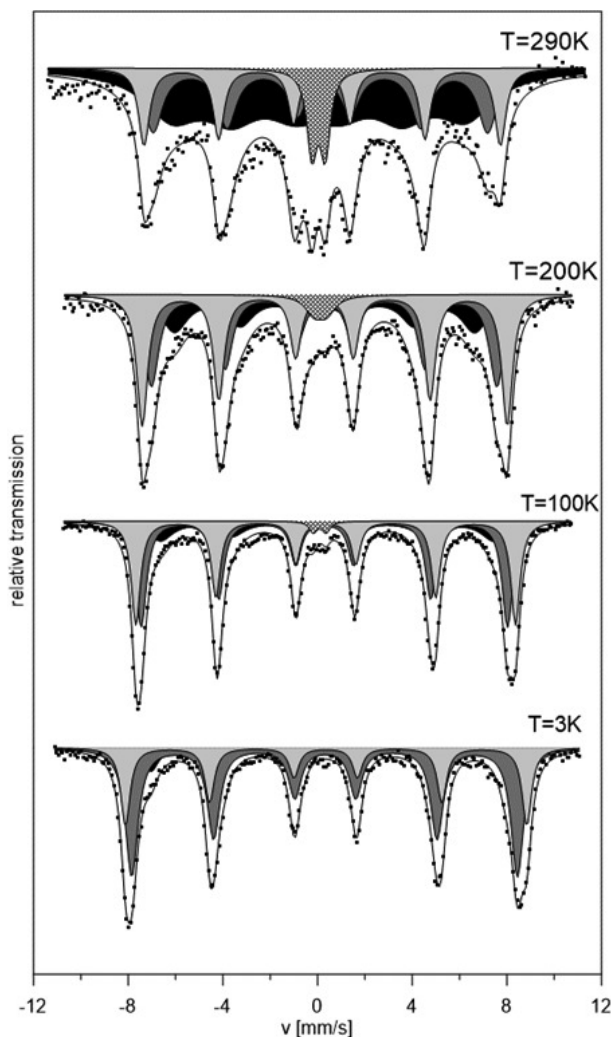


Fig. 3. ⁵⁷Fe Mössbauer spectra of magnetite nanoparticle at various temperatures.

of octahedral and tetrahedral sites is nearly the same. Additionally, in this pattern, one can see yet another component (about 25%). It can be connected with

disordered nanoparticles surface [13] and/or with magnetic interaction between nanoparticles [14]. The component related to surface atoms increases with increasing temperature. This fact is the result of connecting surface atoms and the organic surfactant DMSA. The thermal fluctuations of this surfactant have an impact on the surface particle disorder. The superparamagnetic doublet component can be observed starting from the temperature of 100 K. This component increases with an increasing temperature (see Table 1).

In the superparamagnetic state, the direction of the magnetization of nanoparticles fluctuates among the easy axis of magnetization. These fluctuations can occur in the absence of external magnetic field. The relaxation time τ is the average time required to change the particle magnetization from one direction to another. The relaxation time depends on the kind of nanoparticles, the temperature, and the size of the particle. It is given by the Néel equation in the following form:

$$(3) \quad \tau = \tau_0 \exp \frac{KV}{k_B T}$$

where K is the anisotropy constant of the particle, V is the particle volume, k_B is the Boltzmann constant, and T is the temperature. τ_0 is a constant and equal to about 10^{-10} s.

The superparamagnetic relaxation of magnetite nanoparticles are correlated with the particle volume and the temperature. At RT, the superparamagnetic phase component is the biggest. When the temperature is reduced, the superparamagnetic fluctuation is blocked. Below 100 K, the doublet component disappears and only the sextet pattern remains.

The result of calorimetric experiment is shown in Fig. 4, in which the temperature rise is presented as the function of time. In our case, the magnetic field strength (H_{\max}) was 10.3 kA/m, and the frequency (f) was 257 kHz. The sample was heated for about 53 min and it reached the temperature of 48°C.

Table 1. The hyperfine interactions parameters of the ⁵⁷Fe Mössbauer spectra of Fe₃O₄ determined at different temperatures

Temperature [K]	Subspectra	Rel. int. [%]	IS [mm/s]	B [T]	QS [mm/s]
290	Octahedral sites	17.7	0.19	46.6	0.01
	Tetrahedral sites	22.2	0.20	44.1	-0.07
	Disordered surface	53.2	0.29	<39.3>	0.037
	Superparamagnetic	6.9	0.05	-	0.276
200	Octahedral sites	36.7	0.30	47.8	0.01
	Tetrahedral sites	34.8	0.30	45.3	-0.05
	Disordered surface	25.2	0.36	<39.5>	-0.05
	Superparamagnetic	3.4	0.12	-	0.27
100	Octahedral sites	36.7	0.34	49.7	-0.005
	Tetrahedral sites	43.4	0.31	47.8	-0.007
	Disordered surface	18.4	0.40	<43.6>	-0.04
	Superparamagnetic	1.5	0.44	-	-0.03
3	Octahedral sites	27	0.35	52.5	0.008
	Tetrahedral sites	60	0.32	50.5	-0.016
	Disordered surface	13	0.42	<46.4>	0.038

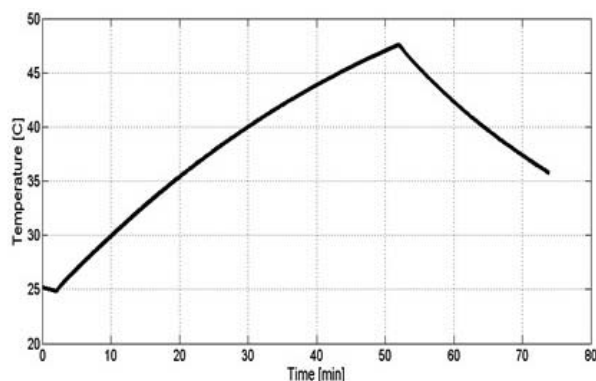


Fig. 4. Temperature rise as a function of time for the commercial ferrofluid ($H_{\max} = 10.3$ kA/m, $f = 273$ kHz).

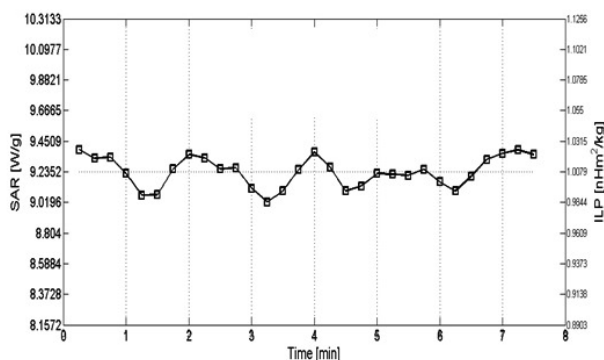


Fig. 5. SAR and ILP values for the sample determined by the corrected slope method within the linear loss region in Fig. 4.

After that time, the magnetic field was switched off and the sample started to cool down. Taking into account the linear part of the heating curve from Fig. 4 (7.5 min in our case), the SAR and ILP parameters were evaluated (see Fig. 5) using the corrected slope method [10].

Conclusions

In this work, the commercial DMSA-coated magnetite nanoparticles were analysed. The average size of MNPs obtained based on the XRD pattern analysis (12.3 nm) and size distribution from TEM images (11.4 nm) is slightly larger than that declared by the manufacturer (10.3 nm). In these nanoparticles, the superparamagnetism phenomenon is observed above 100 K. The average blocking temperature, which is defined as the temperature at which 50% of the magnetically ordered components area has collapsed, is above RT.

The studied nanoparticles can be applied in hyperthermia because they effectively give off heat to the system under the influence of alternating magnetic field. The calculated SAR value from calorimetric measurement is equal to 9.24(11) W/g and the ILP is equal to 1.01(1) nHm²/kg.

References

- Berry, C. C., & Curtis, A. S. G. (2003). Functionalisation of magnetic nanoparticles for applications in biomedicine. *J. Phys. D-Appl. Phys.*, 36(13), 198–206.
- Subramanian, M., Miaskowski, A., Pearce, G., & Dobson, J. (2016). A coil system for real-time magnetic fluid hyperthermia microscopy studies. *Int. J. Hyperthermia*, 32(2), 112–120.
- Chudzik, B., Miaskowski, A., Surowiec, Z., Czernel, G., Duluk, T., Marczuk, M., & Gagoś, M. (2016). Effectiveness of magnetic fluid hyperthermia against *Candida albicans* cells. *Int. J. Hyperthermia*, 32(8), 842–857. <http://dx.doi.org/10.1080/02656736.2016.1212277>.
- Wang, Z., & Cuschieri, A. (2013). Tumour cell labelling by magnetic nanoparticles with determination of intracellular iron content and spatial distribution of the intracellular iron. *Int. J. Mol. Sci.*, 14, 9111–9125. DOI: 10.3390/ijms14059111.
- Tieyu, C., Xing, P., & Henry, D. (2016). Construction of site-specific core-shell structured nanocomposite for pH-controlled drug delivery. *J. Porous Mater.*, 23, 987–995. DOI: 10.1007/s10934-016-0156-5.
- Johannsen, M., Gneveckow, U., Eckelt, L., Feussner, A., Waldöfner, N., Scholz, R., Deger, S., Wust, P., Loening, S. A., & Jordan, A. (2005). Clinical hyperthermia of prostate cancer using magnetic nanoparticles: Presentation of a new interstitial technique. *Int. J. Hyperthermia*, 21, 637–647. DOI: 10.1080/02656730500158360.
- Carrey, J., Mehdaoui, B., & Respaud, M. (2011). Simple models for dynamic hysteresis loop calculations of magnetic single-domain nanoparticles: Application to magnetic hyperthermia optimization. *J. Appl. Phys.*, 109, 083921-1–083921-17. DOI: 10.1063/1.3551582.
- Liquids Research Limited. (2011). Available from <http://liquidsresearch.com>.
- MagneTherm™ systems. Available from <http://www.nanothermics.com>.
- Wildeboer, R. R., Southern, P., & Pankhurs, Q. A. (2014). On the reliable measurement of specific absorption rates and intrinsic loss parameters in magnetic hyperthermia materials. *J. Phys. D-Appl. Phys.*, 47, 495003. DOI: 10.1088/0022-3727/47/49/495003.
- Calero, M., Chiappi, M., Lazaro-Carrillo, A., Rodríguez, M. J., Chichón, F. J., Crosbie-Staunton, K., Prina-Mello, A., Volkov, Y., Villanueva, A., & Carrascosa, J. L. (2015). Characterization of interaction of magnetic nanoparticles with breast cancer cells. *J. Nanobiotechnol.*, 13, 16. DOI: 10.1186/s12951-015-0073-9.
- Williamson, G. K., & Hall, W. H. (1952). X-ray line broadening from filed aluminium and wolfram. *Acta Metallurgica*, 1, 22–31. DOI: 10.1016/0001-6160(53)90006-6.
- Kalska-Szostko, B., Zubowska, M., & Satuła, D. (2006). Studies of the magnetite nanoparticles by means of Mössbauer spectroscopy. *Acta Phys. Pol. A*, 109, 365–369.
- Mørup, S., Hansen, M. F., & Frandsen, C. (2010). Magnetic interactions between nanoparticles. *Beilstein J. Nanotechnol.*, 1, 182–190. DOI: 10.3762/bjnano.1.22.